



Numerical Investigation of EDS Maglev Systems in Terms of Performance and Cost for Different PMs-Aluminum Rail Arrangements

Hakki Mollahasanoglu^{1,2} · Murat Abdioglu^{2,3} · Ufuk Kemal Ozturk² · Halil Ibrahim Okumus⁴ · Elvan Coskun⁵ · Ali Gencer⁵

Received: 17 September 2024 / Accepted: 29 December 2024 / Published online: 10 January 2025
© The Author(s), under exclusive licence to Springer Science+Business Media, LLC, part of Springer Nature 2025

Abstract

Permanent-magnet electro-dynamic suspension (PMs-EDS) maglev systems are shaping the future of modern transport by providing high-speed, energy-efficient, and sustainable transport solutions. In this study, numerical simulations were performed to determine the optimum geometrical parameters of aluminum rail and permanent magnet arrangements for EDS systems. For that, the aluminum rail and permanent magnet combinations were investigated, and then the same simulations were repeated by creating cavities in the aluminum rails for cost efficiency. The highest levitation-to-drag ratio (LDR) was achieved with magnet arrays having a fill factor of 0.4, 20 mm thick aluminum, and an aluminum rail width of 60 mm. Additionally, by creating cavities into the rails, it was calculated that approximately \$2.44 million could be saved from the total cost of \$17.34 million cost of the 1000 km double-strip aluminum rails, with negligible reduction in the LDR ratio. The findings of this study provide a sustainable and economical transport solution by increasing the cost effectiveness of PMs-EDS maglev systems. The results obtained may pave the way for the development of different types of applications of maglev technology and increase the potential for commercial use of maglev transport systems.

Keywords Magnetic levitation · Electrodynamic suspension (EDS) · Permanent magnet (PM) · PM-EDS

1 Introduction

Maglev systems are an important component of modern transport with the potential to provide frictionless and fast transport. They are based on two basic technologies, electromagnetic suspension (EMS), and electrodynamic suspension (EDS). EMS allows the train to rise using

electromagnets with magnetic rails, which offer precise control and energy efficiency. Many investigations have been conducted on the EMS maglev system [1, 2] including optimizing magnetic levitation control parameters [3], investigating motor types [4], or developing test systems [5–7]. However, EDS offers a more stable structure at high speeds and uses superconducting or permanent

✉ Hakki Mollahasanoglu
hakki.mollahasanoglu@erdogan.edu.tr

✉ Ufuk Kemal Ozturk
kozturk@ktu.edu.tr

Murat Abdioglu
muratabdioglu61@gmail.com

Halil Ibrahim Okumus
okumus@ktu.edu.tr

Elvan Coskun
elvncoskun@ankara.edu.tr

Ali Gencer
ali.gencer@science.ankara.edu.tr

¹ Department of Electrical-Electronics Engineering, Faculty of Engineering and Architecture, Recep Tayyip Erdoğan University, Rize, Turkey

² Electromagnetic Guidance and Acceleration Research Group (EMGA), Department of Physics, Faculty of Science, Karadeniz Technical University, 61080 Trabzon, Turkey

³ Department of Mathematics and Science Education, Faculty of Education, Bayburt University, 69000 Bayburt, Turkey

⁴ Department of Electrical-Electronics Engineering, Faculty of Engineering, Karadeniz Technical University, 61080 Trabzon, Turkey

⁵ Center of Excellence for Superconductivity Research, 50, Year Campus, 06830 Golbasi, Ankara, Turkey

magnets that allow the train to levitate naturally when a certain speed is exceeded for the train to move. Since electrodynamic levitation provides levitation without contact by utilizing the natural repulsive forces of magnetic fields, it is safer in the event of de-energization and offers more stable travel at higher speeds. Furthermore, the self-stabilizing nature of the EDS as it accelerates allows it to consume less energy at high speeds and require less maintenance. These properties make EDS more advantageous than EMS, especially in long-distance and high-speed railway systems. When the studies on the EDS Maglev system in recent years are examined, it is seen that they are focused on the development and optimization of EDS systems [8], theoretical analyses [9], and simulation and modeling studies [10, 11]. These studies are crucial for understanding the dynamic behavior of the system, optimizing the design of magnetic components and predicting performance under various operating conditions. Advanced computational methods such as finite element analysis (FEA) [12] and computational fluid dynamics (CFD) [13] are used to simulate the electromagnetic interactions and aerodynamic forces acting on the vehicle. These simulations help to determine the optimal configurations for magnets and coils to reduce energy consumption and improve overall system efficiency.

An important area of research within EDS Maglev systems is the use of permanent magnets (PMs) to provide levitation. PMs-EDS systems utilize the high magnetic field strengths of innovative permanent magnets such as NdFeB to generate the required lift forces. Furthermore, the use of permanent magnets reduces energy consumption and lowers the maintenance costs of the system because it does not require continuous energy like electromagnets. They also offer lower energy consumption compared to superconducting magnets and lower operating costs as they do not require cryogenic cooling. Recent studies on PMs-EDS have investigated various configurations [14] and materials [15] to improve the performance and feasibility of these systems. These studies have investigated the optimal arrangement of magnets and coils, the effect of different guide materials, and the effects of temperature variations on magnetic properties of PMs-EDS.

This study, different from the literature [16], aims to optimize the performance and cost-effectiveness of Maglev systems by introducing a cavities rail structure beyond the discontinuous rail forms in the existing literature. Numerical simulations were performed to determine the optimum system performance and to reduce the total PMs-EDS system cost. These simulations were carried

out in COMSOL Multiphysics 5.6 by using “Magnetic Field Formulation (mf)” physics. In this study, the optimized levitation-to-drag ratio achieved through the voids created in the aluminum rails improves energy efficiency and system stability. Compared to previous configurations in the literature, this study successfully balances cost and performance, supporting the commercial viability of Maglev technology on a large scale. This novel approach provides both sustainable transport solutions and cost-effectiveness in high-speed transport.

2 PMs-EDS System and Numerical Modeling

PMs-EDS systems consist of PMs traveling relative to a fixed conductive guide with an air gap between them. Figure 1 shows the physical model of a PMs-EDS system [17]. The motion of the PMs in the x-axis direction with respect to the conductive layer induces an eddy current in the layer, and the interaction between the PMs magnetic field and the eddy current develops lift and drag forces in the z and x-axis directions, respectively. The vertical force in the z-axis lifts the PMs into a certain air gap, and the drag force in the negative x-axis counteracts the PM's movement.

The behavior of the forces at a certain velocity shown in Fig. 1 can be easily explained for this type of rail. Hence, the drag and lift forces are expressed as shown in Eqs. 1 and 2 [18].

$$F_z = F_L = \frac{B_0^2 w \rho \tau}{\mu_0} \frac{1}{\beta \eta + 1} e^{-2\beta h} \quad (1)$$

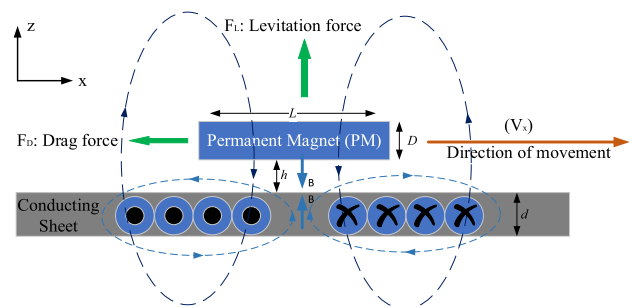


Fig. 1 Physical model of EDS systems

$$F_x = F_D = \frac{B_0^2 w \rho \tau}{\mu_0} \frac{\beta \eta}{\beta \eta + 1} e^{-2\beta h} \quad (2)$$

where μ_0 is the vacuum permeability, B_0 is the flux density peak value of the permanent magnet array, w is the width of the permanent magnets, ρ is the number of the pair magnet poles, τ is the pole pitch of permanent magnets, $\beta = \pi/\tau$, h is the suspension gap, $\eta = \sqrt{\lambda/\pi\mu\sigma v}$ is the skin depth, μ is the plate permeability, $\lambda = 2\tau$ is the magnet wavelength, σ is the plate conductivity, and v is the PM (magnetic source) velocity.

There is an important parameter widely used in literature to evaluate the performance of such systems. This is the lift-to-drag ratio, expressed as LDR, which is an indicator of the efficiency of the suspension at a given speed. Therefore, LDR can be defined as,

$$LDR = \frac{F_{\text{lift}}}{F_{\text{drag}}} = \frac{1}{\beta \eta} = \frac{1}{2\pi} \sqrt{\pi \mu \sigma \lambda v} \quad (3)$$

In the scope of this study, the topology given in Fig. 2 has been created. Calculations were made in the COMSOL program by defining a 1 mm thick calculation domain around the upper PM array (shown in Fig. 2a with red dashed line). The upper PM array is adjusted to coincide

Table 1 Physical parameters of PMs-EDS system for numerical calculations

Parameter	Description	Value
len_Hpm	Length PM (x)	30 mm
w_Hpm	Width PM (y)	30 mm
t_Hpm	Height PM (z)	30 mm
len_Vpm	Length PM (x)	45 mm
w_Vpm	Width PM (y)	30 mm
t_Vpm	Height PM (z)	30 mm
len_Al	Length of aluminum rail	1200 mm
l_Al_ladder	Length of a ladder	60 mm
wAl_out	Width of aluminum rail	40–60 mm
t_Al	Thickness of aluminum rail	5–25 mm

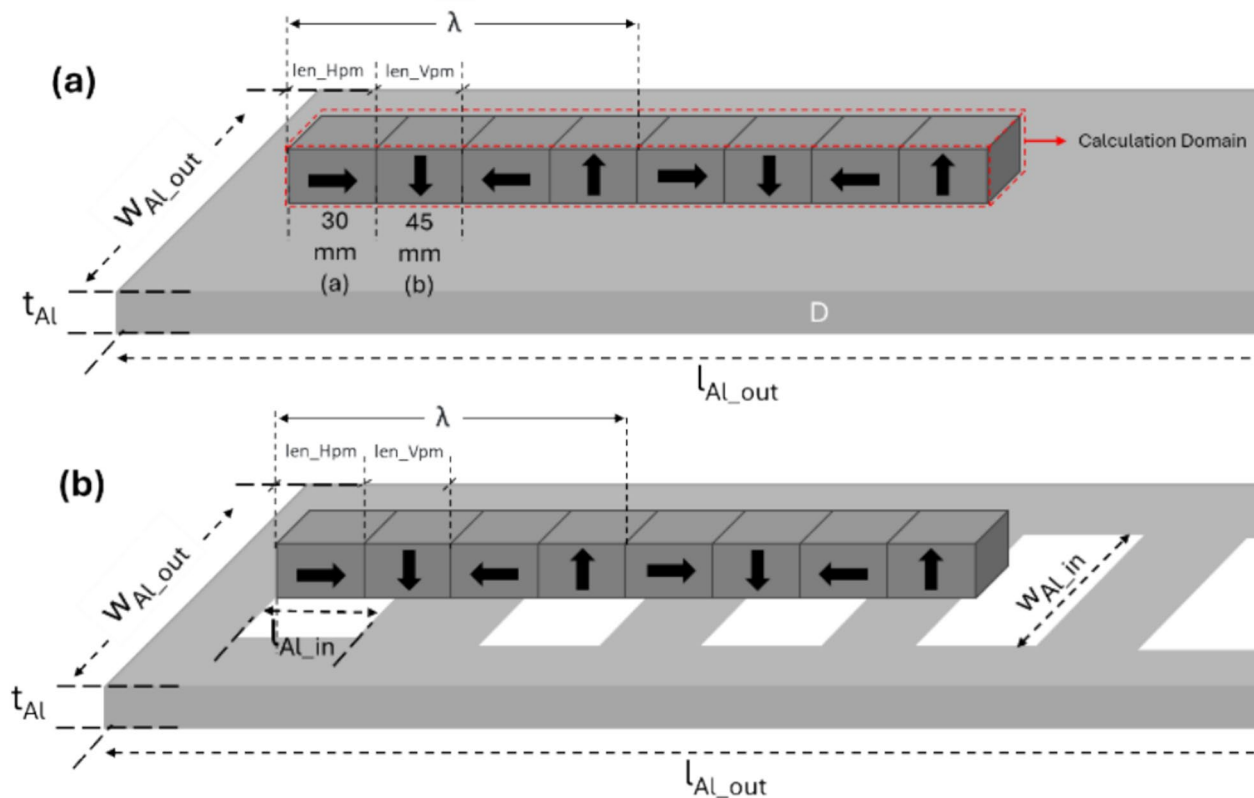


Fig. 2 Schematic illustration of Maglev dynamic levitation concept with full (a) and periodically cavitied (b) aluminum rail

with the geometric center of the lower aluminum rail. Therefore, the calculations were obtained by considering the per 1200 mm long aluminum rail length specified in Table 1. This calculation domain was used in simulations to calculate both levitation and drag forces.

The numerical simulations were performed in “Magnetic Field Formulation (mfh)” physics in COMSOL Multiphysics 5.6. In the modeling, the magnetization directions and magnetic field values of the PMs are defined by Faraday’s law while the velocity up to 1100 km/h is defined by Lorentz Term. This study focuses on the impact and cost analysis of different aluminum rail arrangements on EDS Maglev Systems at 100 m/s operating speed. The main reason why the speed of 100 m/s was preferred in our study is that this speed is both a suitable reference for evaluating the optimum performance of EDS systems and for the speeds in commercial transport applications. At this speed, the relationship between magnetic lift and drag forces and LDR values can be clearly analyzed and the results become comparable with other maglev and high-speed train studies.

Table 1 shows the physical parameters of the permanent magnet and aluminum rail.

In this study, the remanent magnetization value of each magnet was taken as $B_r = 1.42$ T and the electrical conductivity value of aluminum rail was taken as $\sigma = 3 \times 10^7$ S/m.

The magnetic force performance and cost analyses of the PMs-EDS system using full and cavitated aluminum rail are investigated. For this purpose, the work steps were listed as follows:

- Determination of the optimum fill factor
- Determination of optimum aluminum rail thickness and width
- Determination of levitation and drag forces by creating cavities with different dimensions in the aluminum rail
- Cost analysis of PMs-EDS systems

Table 2 PMs dimensions and corresponding fill-factors

len_Hpm (mm)	len_Vpm (mm)	Wavelength, λ (mm)	Fill-factor (γ)
7.5	67.5	150	0.10
10	65	150	0.13
15	60	150	0.20
20	55	150	0.27
25	50	150	0.33
30	45	150	0.40
37.5	37.5	150	0.50
45	30	150	0.60
55	20	150	0.73

3 Results and Discussions

In the modeling, the optimum fill factor (γ) value is determined first. The fill factor (see Fig. 2) can be defined as the ratio of the length of horizontal PMs to the wavelength (λ) as given in Eq. 4.

$$\gamma = \frac{2a}{2(a+b)} = \frac{a}{0.5\lambda} \quad (4)$$

The values of levitation and drag forces and related LDR ratio at the maximum velocity of 100 m/s for different fill factors shown in Table 2 are given in Fig. 3.

The optimum fill factor was determined as 0.40 because the levitation force is the highest and the drag force is moderate at this value. This fill factor value is used for the simulations in the rest of this paper with PM arrays that consist of 8 PMs as shown in Fig. 2.

Levitation and drag force values depending on velocity were calculated for different aluminum thicknesses (5, 8,

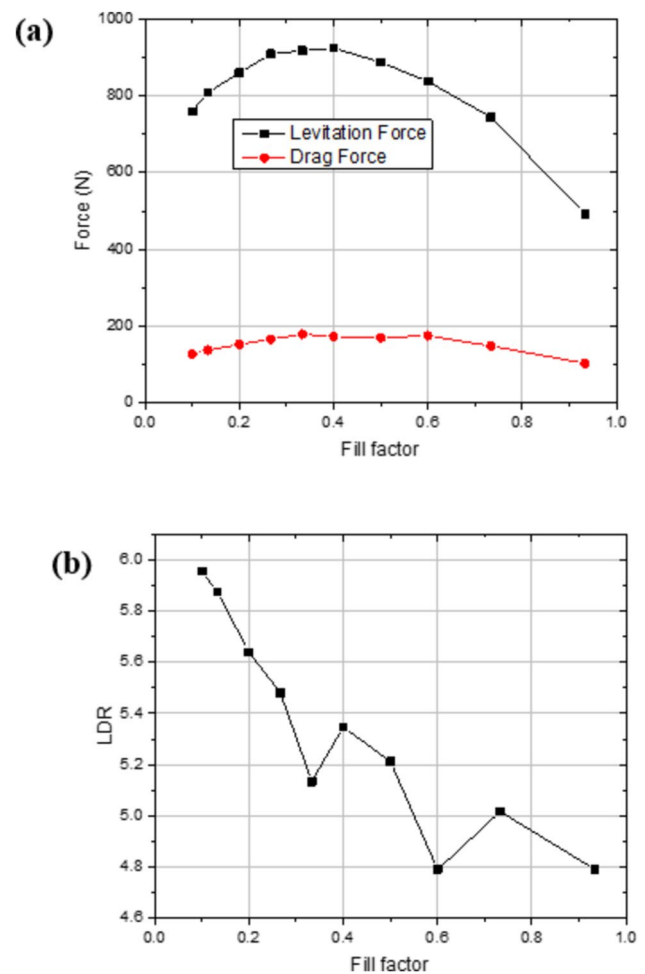


Fig. 3 The levitation and drag forces at the maximum velocity of 100 m/s (a) and lift-to-drag ratio (LDR) (b) depending on the fill factor of the PMs array consisted of 5 PMs

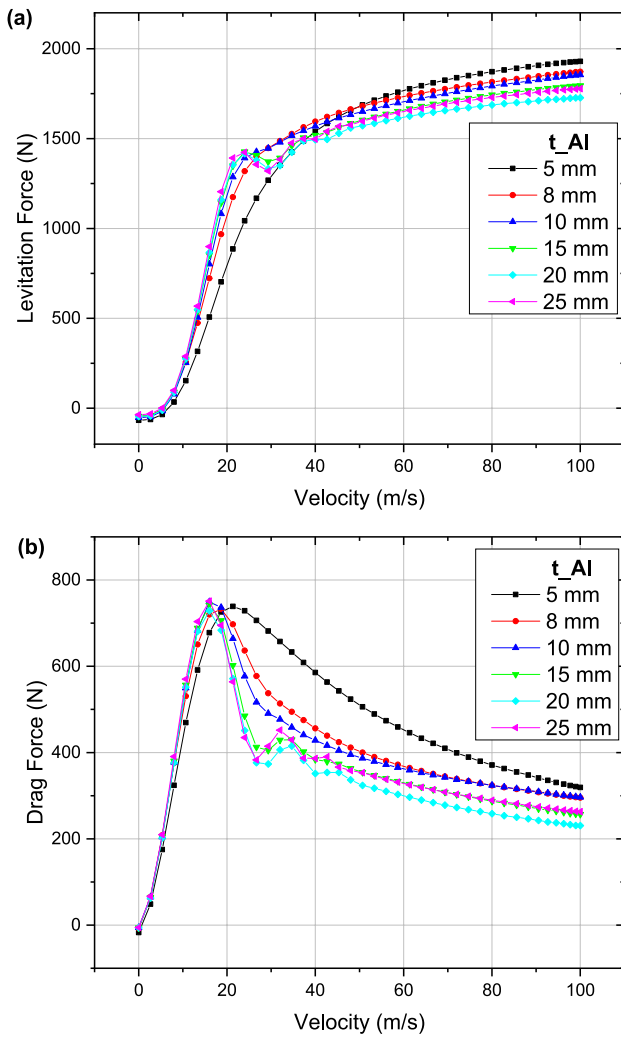


Fig. 4 The levitation (a) and drag (b) force curves between the PMs and of different thickness of aluminum rail

10, 15, 20, and 25 mm) to determine the optimum thickness of the aluminum rail. The results obtained are given in Fig. 4.

As shown in Fig. 4a, as the speed increases, the value of η given in Eq. 1 decreases and thus the levitation force increases. Also, it is seen from Fig. 4b that the drag force value first increases and then decreases depending on the decreasing η value with increasing speed in Eq. 2.

In order to determine the optimum aluminum thickness accurately, the variation of magnetic force (levitation and drag force) and LDR values depending on the aluminum thickness is plotted in Fig. 5 using Fig. 4.

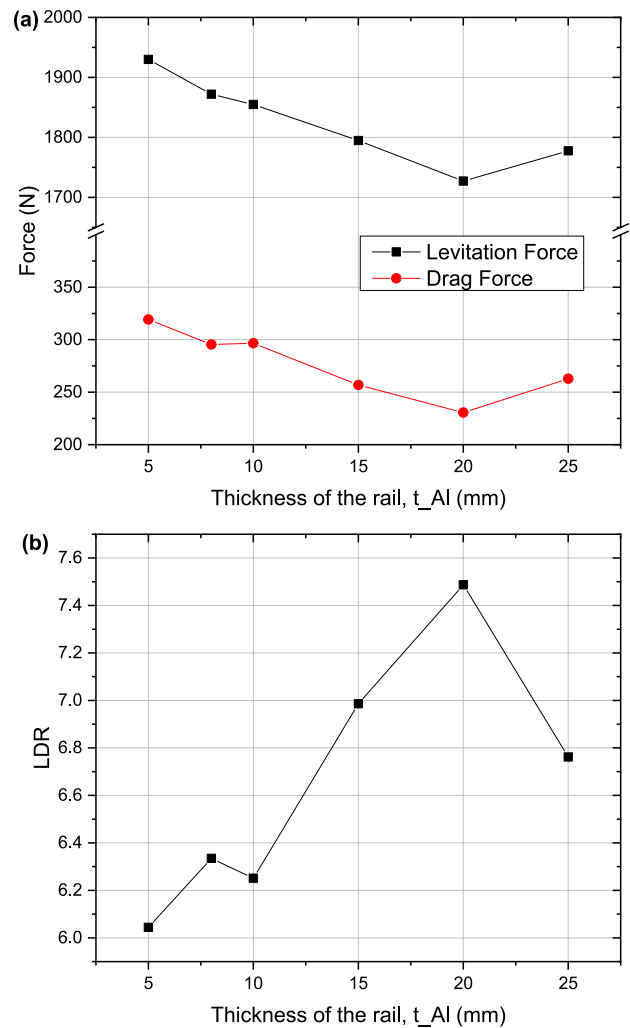
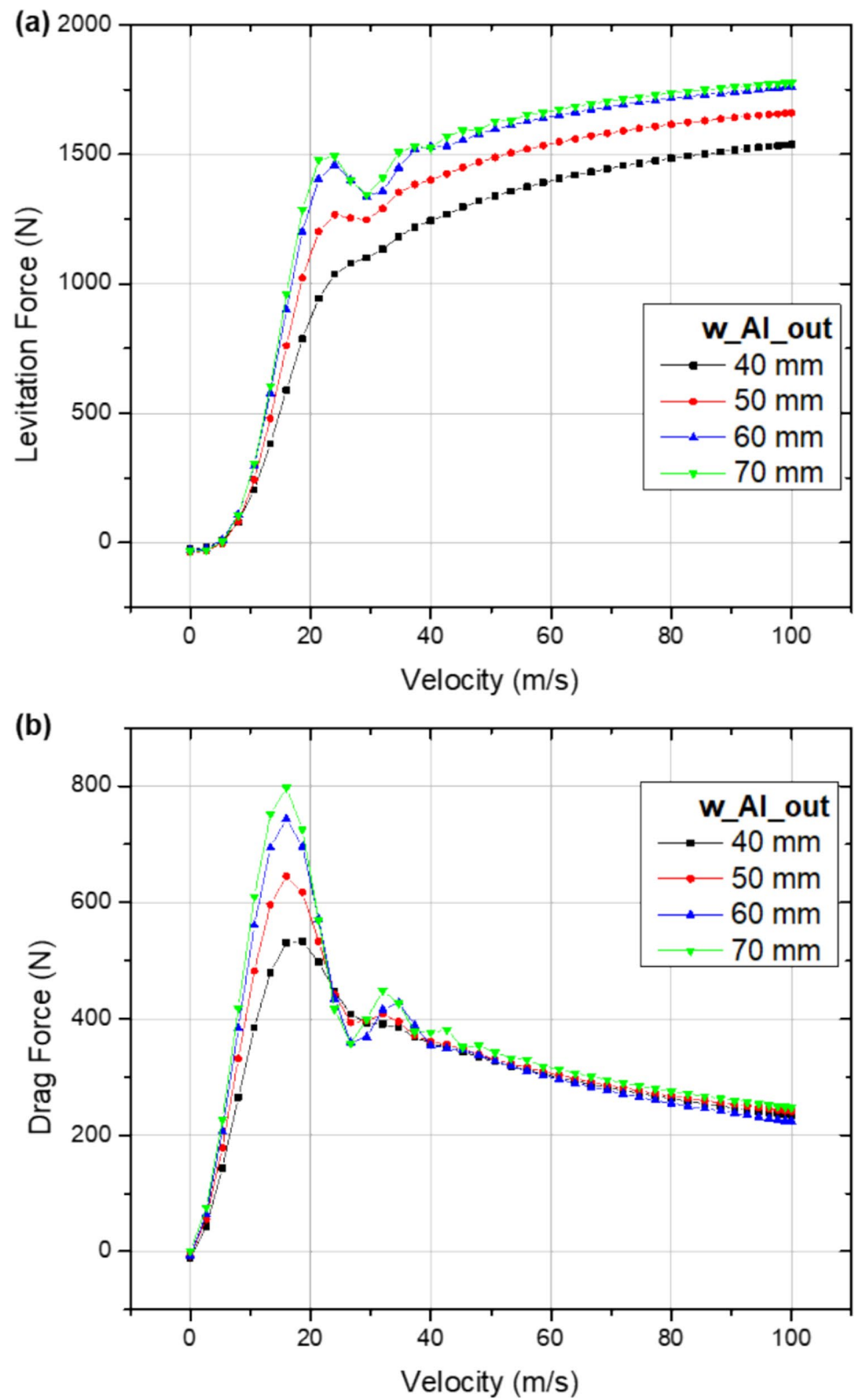


Fig. 5 The levitation and drag forces at the maximum velocity of 100 m/s (a) and lift-to-drag ratio (LDR) (b) depending on the thickness of the aluminum rail

The optimum aluminum rail thickness was determined as 20 mm as shown in Fig. 5, because this value is the point with the highest LDR value and lowest drag force value. The variation of the LDR values as a function of rail thickness in Fig. 5 shows that the relative bulk conductivity of the aluminum rail, σ (see Eq. 3), varies with aluminum thickness and the wavelength and thickness of the interacting magnet. The lower drag force value is important in terms of reducing the instantaneous energy consumption during traveling at high speeds due to lower braking forces as relationship $P = vF_{drag}$. Therefore, this thickness value is used for the simulations in the rest of this paper.

Fig. 6 The levitation (a) and drag (b) force curves between the PMs and aluminum rail of different width



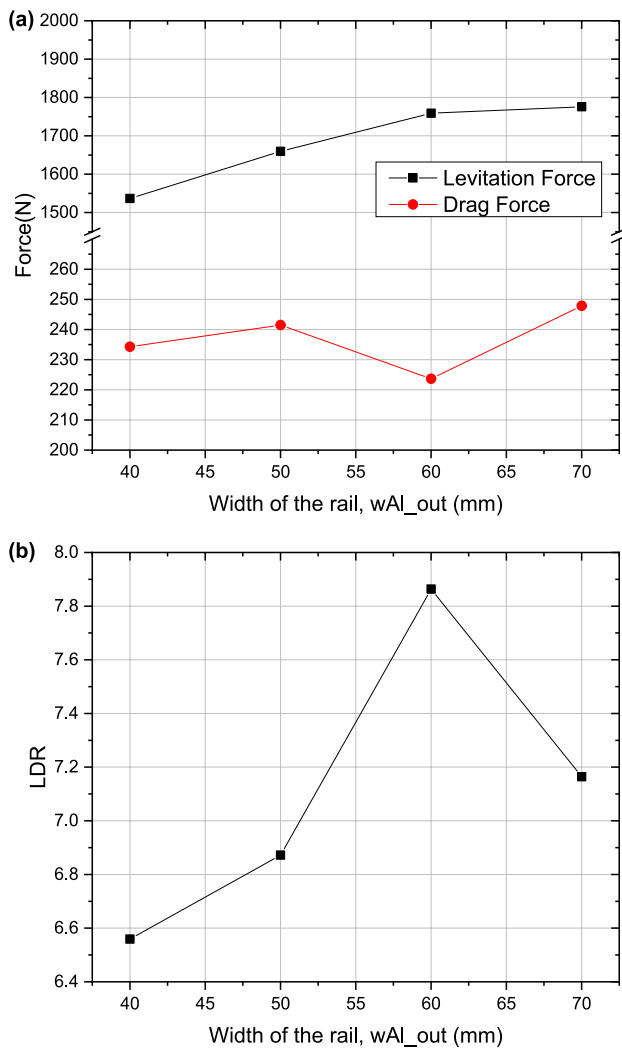


Fig. 7 The levitation and drag forces at the maximum velocity of 100 m/s (a) and lift-to-drag ratio (LDR) (b) depending on the width of the aluminum rail

After determining the optimum rail thickness, numerical simulations were carried out to determine the optimum width of the aluminum rail. The results obtained are given in Fig. 6.

In order to determine the optimum aluminum width accurately, the variation of magnetic force and LDR values depending on the aluminum width is plotted in Fig. 7 using Fig. 6 at 100 m/s speed.

Considering Fig. 7, the optimum rail width was determined as 60 mm because the LDR has its maximum value

at this point. This value will be used for the simulations in the rest of this paper.

After determining the optimum thickness and width of the aluminum sheet, it was aimed to reduce the cost by creating cavities on the aluminum sheet. Therefore, cavities of different lengths and widths were created on the aluminum plate and numerical calculations were repeated to determine the effect of the created cavities on the dynamic performance of the Maglev train (levitation and drag force, LDR). Firstly, the levitation and drag forces were calculated for different cavity widths (W_{Al_in}) of 6, 12, 18, 24, 30, and 36 mm (see also Fig. 2b). The results obtained are given in Fig. 8.

To enhance the reliability of the findings, Fig. 9 plots the variation of magnetic force and LDR values with respect to cavity width, utilizing the data from Fig. 8 at a speed of 100 m/s.

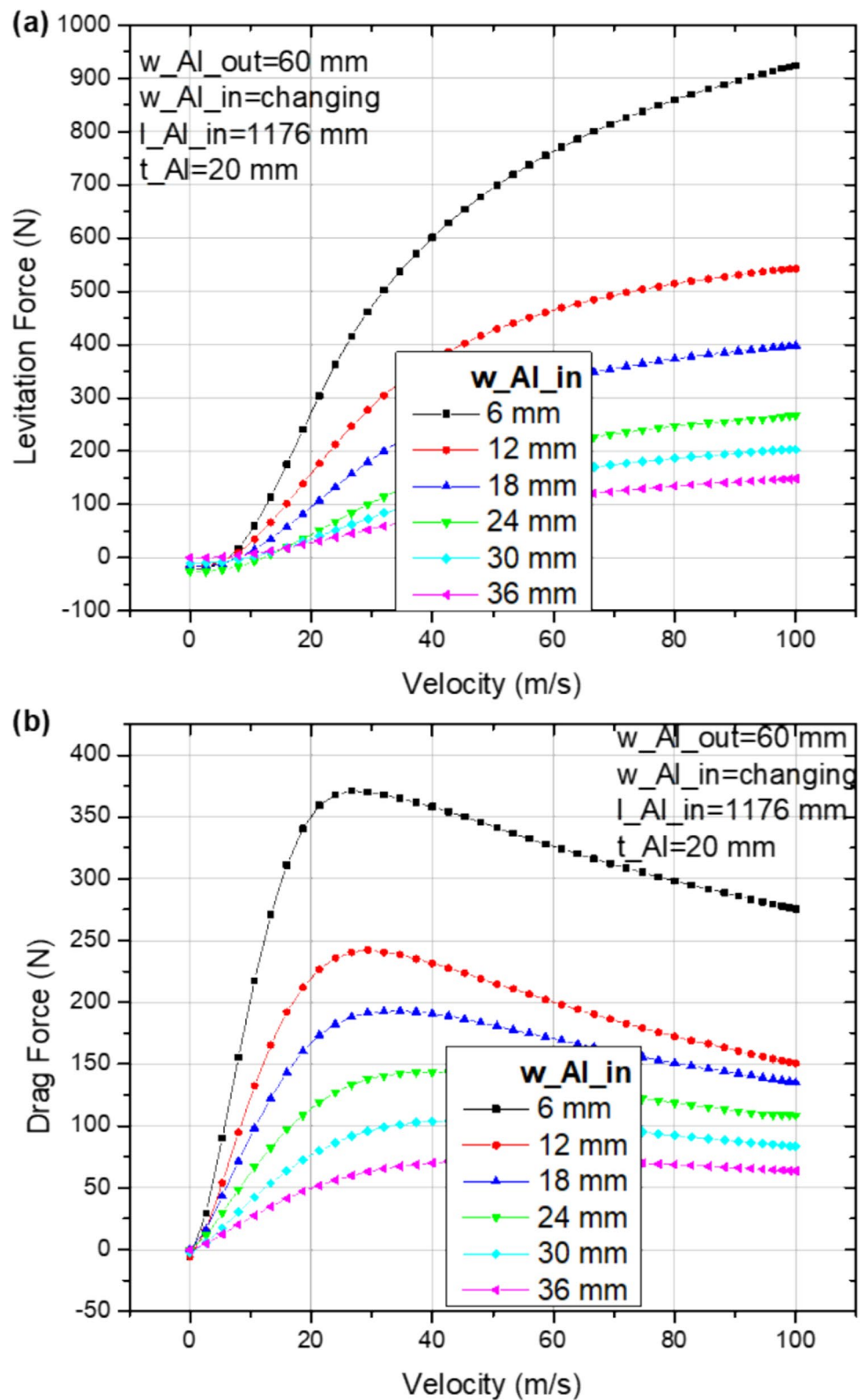
Based on the results from Fig. 9, we performed additional measurements, selecting three values as 6 mm, 12 mm, and 36 mm to make a more accurate comparison and to obtain high performance and low cost in terms of PMs-EDS systems. For that unit length of the ladder (l_{Al_ladder}) was chosen as constant of 60 mm, shown in Fig. 2b. Subsequent, numerical simulations were then performed to determine the optimal lengths of cavities in aluminum rail (l_{Al_in}). As seen in Fig. 9, despite the decrease in levitation force, the LDR value shows a slight increase. This phenomenon can be explained by the definition of the LDR, which is calculated as the ratio of the levitation force to the drag force (Eq. 3). Figures 10, 11, and 12 show the magnetic force and LDR values for different volumes of cavities formed on the aluminum layer.

When Figs. 10, 11, and 12 are analyzed together, it is seen that the drag force increases when the length of the cavity (l_{Al_in}) is 2 mm. This shows that the length of the cavity creates an additional resistance on the system. Accordingly, it is observed that the LDR value also decreases. In addition, when Figs. 10, 11, and 12b are analyzed, it is observed that when the length of the cavity is 12 mm, the LDR value increases compared to the previous values, although the void amount increases.

Using the data in these graphs, the cost for each topology was calculated and Fig. 13 was created. Figure 13 shows the plot of the LDR/cost ratio versus cavity length. The aim here is to achieve high levitation performance at low cost in PMs-EDS systems.

The LDR/cost ratio here is the ratio of the LDR value of the relevant length of the cavity aluminum to the price in dollars of a 1.2 m long aluminum rail (with topologies of

Fig. 8 The levitation (a) and drag (b) force curves between the PMs and aluminum rail with different widths of cavity (w_{Al_in}). The length of the cavity is 1176 mm corresponding to 98% of the total rail length



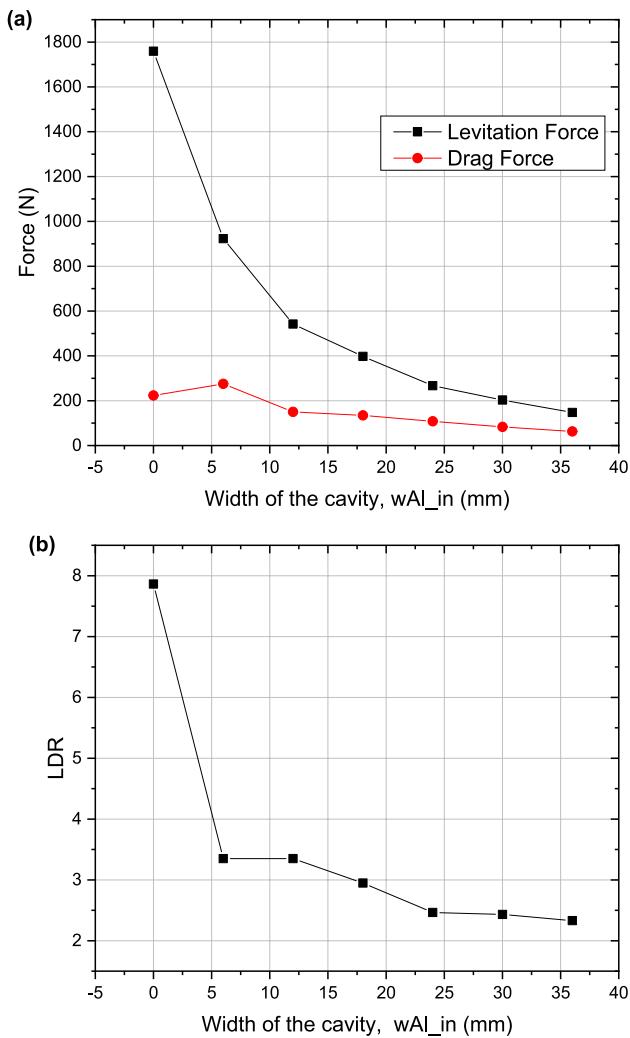


Fig. 9 The levitation and drag forces at the maximum velocity of 100 m/s (a) and lift-to-drag ratio (LDR) (b) depending on the width of the cavity (w_{Al_in}) in the aluminum rail

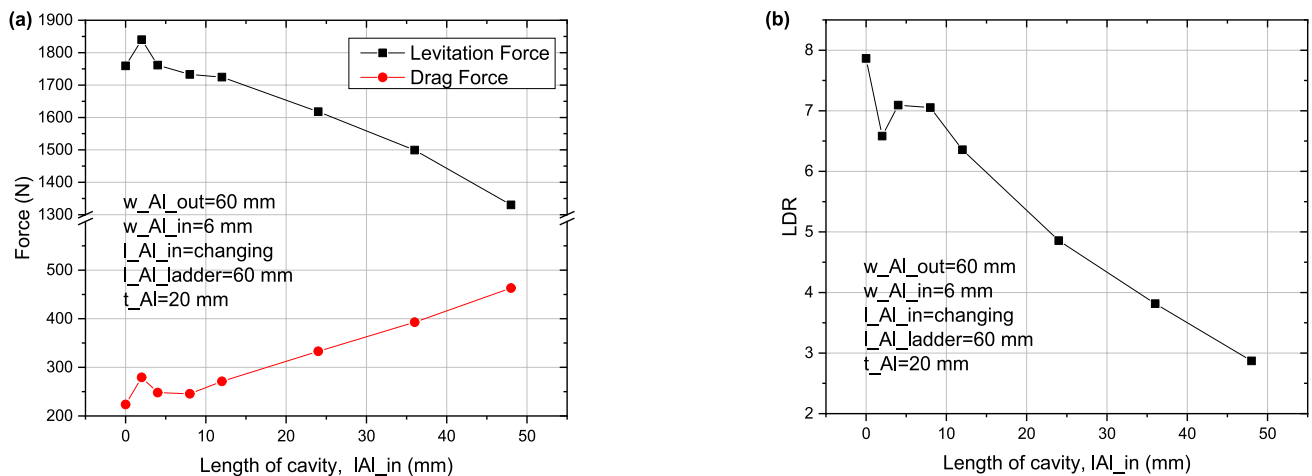


Fig. 10 The levitation and drag forces at the maximum velocity of 100 m/s (a) and lift-to-drag ratio (LDR) (b) depending on the length of the cavity (l_{Al_in}) in the aluminum rail. The width of the cavity is 6 mm corresponding to 10% of the total rail width

different volumes) in the numerical calculation area. In the cost calculation, the price of 1 kg of aluminum ingot is taken as 2.67 USD [19].

When Fig. 13 is examined, it is seen that the LDR/cost ratios of the ladder aluminum layer are higher for all lengths of the cavity value when the width of the cavity (w_{Al_in}) is 12 mm.

In addition, when the case where $w_{Al_in} = 36$ mm is analyzed, it is seen that the LDR/cost ratio at the $l_{Al_in} = 12$ mm point is larger than the other l_{Al_in} cases. The cost of a 1000 km double lanes aluminum track without any cavity is 17.34 million dollars ($l_{Al_in} = 0$). When $l_{Al_in} = 12$ mm, the money saved due to the removed aluminum (cavity) is 834 thousand dollars for $w_{Al_in} = 12$ mm, while it is approximately 2.44 million dollars for $w_{Al_in} = 36$ mm. This shows that although the LDR/cost ratio $w_{Al_in} = 12$ seems to be higher, when the money saved is considered, $l_{Al_in} = 36$ is more suitable for PMs-EDS systems.

4 Conclusion

This study has performed extensive numerical simulations to determine the optimum geometrical parameters of aluminum rail and permanent magnet arrangements to achieve higher lift and lower drag forces in maglev systems. In the first stage, the performance of the systems arranged with aluminum rails at the bottom and permanent magnets at the top was examined, and then the same simulations were repeated by creating cavities in the aluminum rails for cost efficiency.

The maximum levitation to drag ratio was obtained when the fill factor of the magnet arrays forming the magnetic field source was 0.4, the aluminum thickness

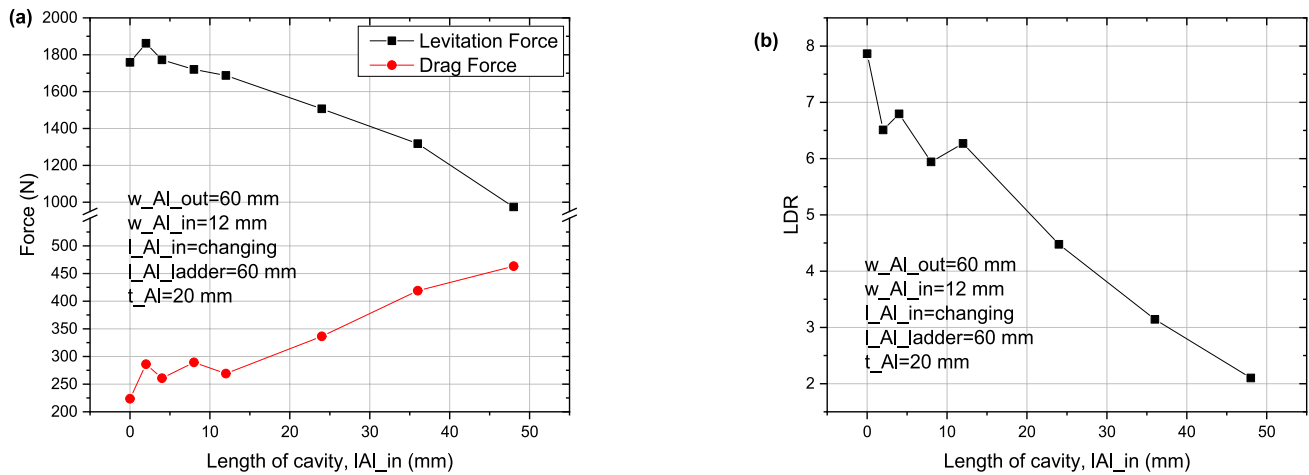


Fig. 11 The levitation and drag forces at the maximum velocity of 100 m/s (a) and lift-to-drag ratio (LDR) (b) depending on the length of the cavity (l_{Al_in}) in the aluminum rail. The width of the cavity is 12 mm corresponding to 20% of the total rail width

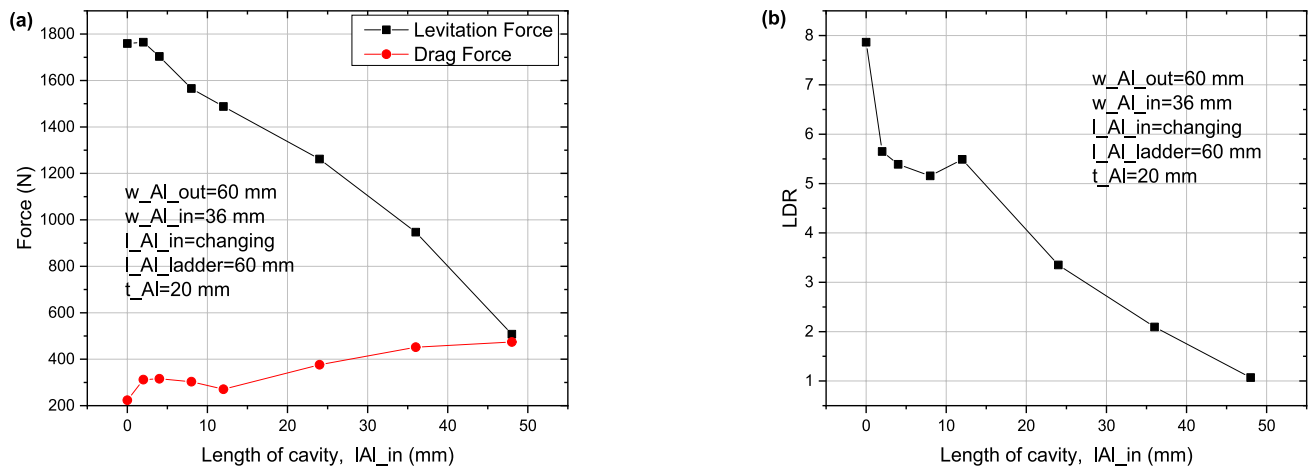


Fig. 12 The levitation and drag forces at the maximum velocity of 100 m/s (a) and lift-to-drag ratio (LDR) (b) depending on the length of the cavity (l_{Al_in}) in the aluminum rail. The width of the cavity is 36 mm corresponding to 60% of the total rail width

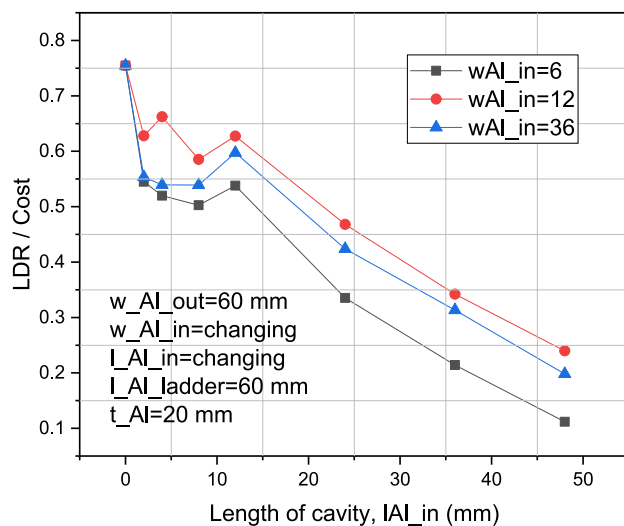


Fig. 13 LDR/cost ratio depending on the length of the cavity (l_{Al_in}) in the aluminum rail for different widths of cavity (w_{Al_in})

was 20 mm, and the aluminum rail width w_{Al_in} was 60 mm. In addition, it has been determined that a saving of approximately 2.44 million dollars will be achieved when the numeric calculation is made by creating cavities in the rails without much reduction in the LDR ratio in a 1000 km double strip aluminum rails with a total cost of 17.34 million dollars.

The results of this study have the potential to improve the cost-effectiveness of PMs-EDS maglev systems and provide a more sustainable and economical transport solution. Furthermore, this numerical calculation by creating voids in aluminum rails contributes to the development of innovative approaches in the fields of engineering and materials science. Future studies will carry these findings to wider applications, enabling important steps to be taken towards the widespread use of maglev technology and increasing its efficiency.

Acknowledgements This study was supported by the Scientific and Technological Research Council of Turkey (TUBITAK) under project number 122F432 and Karadeniz Technical University Scientific Research Projects Coordination Unit under project number FBA-2021-9814 and FBA-2024-16040.

Author Contributions HM and UKO wrote the main text of the paper, MA wrote the simulation studies and HIO contributed to the literature review. EC and AG made the necessary corrections. All authors revised the manuscript.

Data Availability No datasets were generated or analysed during the current study.

Declarations

Competing Interests The authors declare no competing interests.

References

- Feng, Y., Zhao, C., Bai, Z., Tong, L., Shu, Y.: A modified electromagnetic force calculation method has high accuracy and applicability for EMS maglev vehicle dynamics simulation. *ISA. Trans.* **137**, 186–198 (2023). <https://doi.org/10.1016/j.isatra.2023.01.019>
- Li, F., Sun, Y., Xu, J., He, Z., Lin, G.: Control methods for levitation system of EMS-type maglev vehicles: an overview. *Energies* **16**, 2995 (2023). <https://doi.org/10.3390/en16072995>
- Wang, M., Zeng, S., He, Y., Su, S., Liu, P.: Multi-objective optimization of a fractional-order control system for an EMS-type maglev model. *IEEE Transactions on Vehicular Technology*. 1–16 (2024). <https://doi.org/10.1109/TVT.2024.3394955>
- Lv, G., Cui, L., Zhi, R., Zhou, T., Liu, Y.: Investigation of the transverse flux linear synchronous motor integrated with propulsion, levitation and guidance for the maglev train. *IEEE. Trans. Electrification*. **9**, 4113–4120 (2023). <https://doi.org/10.1109/TTE.2023.3246070>
- Ozturk, U.K., Abdioglu, M., Mollahasanoglu, H.: Magnetic force performance of hybrid multisurface HTS maglev system with auxiliary onboard PMs. *IEEE Trans. Appl. Supercond.* **33**, 1–6 (2023). <https://doi.org/10.1109/TASC.2023.3237762>
- Lee, C.Y., Jo, J.M., Han, Y.J., Chung, Y.D., Yoon, Y.S., Choi, S., Hwang, Y.J., Jo, H.C., Jang, J.Y., Ko, T.K.: Design, fabrication, and operating test of the prototype HTS electromagnet for EMS-based maglev. *IEEE Trans. Appl. Supercond.* **22**, 3600504–3600504 (2012). <https://doi.org/10.1109/TASC.2012.2186778>
- Celik, S.: Design of magnetic levitation force measurement system at any low temperatures from 20K to room temperature. *J. Alloy. Compd.* **662**, 546–556 (2016). <https://doi.org/10.1016/j.jallcom.2015.11.230>
- Xue, Z., Wei, R., Gao, Y., Ge, Q.: Research on electromagnetic force characteristics based on asymmetric 120° pitch figure-8 coils in EDS system for maglev train. In: Jia, L., Qin, Y., Yang, J., Liu, Z., Diao, L., and An, M. (eds.) *Proceedings of the 6th International Conference on Electrical Engineering and Information Technologies for Rail Transportation (EITRT)* 2023. pp. 422–430. Springer Nature, Singapore (2024)
- Wang, X., Huang, J., Fang, Z.: Research on EDS propulsion characteristics of superconducting high speed maglev train. In: Jia, L., Qin, Y., Liang, J., Liu, Z., Diao, L., and An, M. (eds.) *Proceedings of the 5th International Conference on Electrical Engineering and Information Technologies for Rail Transportation (EITRT)* 2021. pp. 20–28. Springer Nature, Singapore (2022)
- Wang, B., Luo, S., Ma, W., Li, G., Wang, Z., Xu, J., Zhang, X.: A fast dynamic model of a two-sided permanent magnet electrodynamic suspension system in a maglev train. *Proc. Inst. Mech. Eng. Part. F: J. Rail. Rapid. Transit.* **237**, 996–1008 (2023). <https://doi.org/10.1177/09544097231168035>
- Ozturk, U.K., Abdioglu, M., Ozkat, E.C., Mollahasanoglu, H.: Extended 2-D magnetic field modeling of linear motor to investigate the magnetic force parameters of high-speed superconducting maglev. *IEEE. Trans. Appl. Supercond.* **33**, 1–8 (2023). <https://doi.org/10.1109/TASC.2023.3245880>
- Bu, F., Xu, J., Chen, J.: Analytical calculation and experiment of 3-D electromagnetic force of permanent magnet electrodynamic suspension system. In: *2023 IEEE International Magnetic Conference - Short Papers (INTERMAG Short Papers)*. pp. 1–2 (2023)
- Fumeaux, M., Cailleteau, M., Melly, D., Chevaillier, S., Cugnoni, J.: Design and simulation of the electrodynamic suspension of an hyperloop test vehicle. In: *2023 14th International Symposium on Linear Drivers for Industry Applications (LDIA)*. pp. 1–5 (2023)
- Beauloye, L., Dehez, B.: Impact of the magnet span on the forces of electrodynamic suspensions with an alternate permanent magnet arrangement. In: *2022 25th International Conference on Electrical Machines and Systems (ICEMS)*. pp. 1–5 (2022)
- Xiang, Y., Deng, Z., Shi, H., Li, K., Cao, T., Deng, B., Liang, L., Zheng, J.: Design and analysis of guidance function of permanent magnet electrodynamic suspension. *Technologies*. **11**, 3 (2023). <https://doi.org/10.3390/technologies11010003>
- Beauloye, L., Dehez, B.: Permanent magnet electrodynamic suspensions applied to MAGLEV transportation systems: a review. *IEEE. Trans. Trans. Electrification*. **9**, 748–758 (2023). <https://doi.org/10.1109/TTE.2022.3193296>
- Moon, F.C.: *Superconducting levitation: applications to bearings and magnetic transportation*. John Wiley & Sons (2008)
- Post, R.F., Ryutov, D.: *The Inductrack concept: a new approach to magnetic levitation*. Lawrence Livermore National Lab. (LLNL), Livermore, CA (United States) (1996)
- Aluminium PRICE Today | Aluminium Spot Price Chart | Live Price of Aluminium per Ounce | Markets Insider. <https://markets.businessinsider.com/commodities/aluminum-price>

Publisher's Note Springer Nature remains neutral with regard to jurisdictional claims in published maps and institutional affiliations.

Springer Nature or its licensor (e.g. a society or other partner) holds exclusive rights to this article under a publishing agreement with the author(s) or other rightsholder(s); author self-archiving of the accepted manuscript version of this article is solely governed by the terms of such publishing agreement and applicable law.